Electronic phase diagram of the iron-based high-T_c superconductor $Ba(Fe_{1-x}Co_x)_2As_2$ under hydrostatic pressure ($0 \leq x \leq 0.099$)

K. Ahilan,[1] F. L. Ning,[1] T. Imai,[1,2] A. S. Sefat,[3] M. A. McGuire,[3] B. C. Sales,[3] and D. Mandrus[3]
[1]*Department of Physics and Astronomy, McMaster University, Hamilton, Ontario, Canada L8S4M1*
[2]*Canadian Institute for Advanced Research, Toronto, Ontario, Canada M5G1Z8*
[3]*Materials Science and Technology Division, Oak Ridge National Laboratory, Oak Ridge, Tennessee 37831, USA*
(Received 14 April 2009; revised manuscript received 28 May 2009; published 18 June 2009)

We report comprehensive resistivity measurements of single-crystalline samples of the $Ba(Fe_{1-x}Co_x)_2As_2$ high-T_c superconductor under hydrostatic pressure up to 2.75 GPa and over a broad concentration range, $0 \leq x \leq 0.099$. We show that application of pressure progressively suppresses the spin-density wave (SDW) transition temperature, T_{SDW}, in the underdoped regime ($x \lesssim 0.051$). There is no sign of pressure-induced superconductivity in the undoped $BaFe_2As_2$ down to 1.8 K but applied pressure dramatically enhances T_c in the underdoped regime $0.02 \lesssim x \lesssim 0.051$. The effect of pressure on T_c is very small in the optimally and overdoped regimes $0.082 \lesssim x \lesssim 0.099$. As a consequence, the dome of the superconducting phase extends to $x \lesssim 0.02$ under pressure. We discuss the implications of our findings in the context of a possible quantum phase transition between the SDW and superconducting phases.

DOI: 10.1103/PhysRevB.79.214520 PACS number(s): 74.70.−b, 74.62.Fj

I. INTRODUCTION

The superconducting mechanism of the new iron-based high-T_c superconductors[1] is highly controversial. Among the key questions which remain unsolved is whether the conventional phonon mechanism is responsible for the superconductivity. Given that the ground state of the undoped parent phases, such as RFe_2As_2 (R=Ba, Sr, Ca), is magnetically ordered in a commensurate spin density wave (SDW) state,[2–6] it is conceivable that spin fluctuations may be playing a role as a glue of Cooper pairs. Unlike the high-T_c cuprate superconductors, however, the magnetically ordered ground state of the undoped parent phases is not a Mott insulating state, and the electrical resistivity ρ remains finite in the SDW state.[1,7] As little as 2–4 % of electron doping into the FeAs layers alters the nature of the SDW order, as evidenced by the dramatic changes in the ^{75}As and ^{59}Co NMR lineshapes in the ordered state of $Ba(Fe_{1-x}Co_x)_2As_2$.[8] The exact nature of the SDW phase in the presence of doped electrons is not understood very well, but the large distributions of the static hyperfine magnetic field observed by NMR are not consistent with a homogeneous commensurate SDW state.[8] Upon further increasing the level of electron doping to the optimal doping level of 6–8 %, a high-T_c phase emerges with $T_c \lesssim 23$ K.[9–13]

Besides doping, it also turns out that applied pressure can induce superconductivity with T_c as high as ~29 K in the undoped parent phases of RFe_2As_2.[14–19] The existence of the pressure-induced superconducting phase indicates that subtle changes and/or contractions of the structure can switch on superconductivity from a SDW phase. However, the mechanism of pressure-induced superconductivity is very poorly understood, and more detailed studies are required to clarify the effects of applied pressure on the electronic properties of iron-based high-T_c superconducting systems. Most of the past experimental studies of these pressure effects, however, have focused on the optimally doped superconducting phase, or on pressure-induced superconductivity in the undoped parent phase (see Ref. 20 for a review). Only limited experimental studies have been reported for the interplay between the amount of doping and pressure on the RFe_2As_2 systems.[21] In this paper, we will present comprehensive resistivity measurements under hydrostatic pressure for $Ba(Fe_{1-x}Co_x)_2As_2$ single crystals over a wide range of Co concentrations from the undoped (x=0) to overdoped regimes up to x=0.099. Unlike earlier reports of the observation of superconductivity in undoped $BaFe_2As_2$ under pressures applied by anvil cells (which tend to produce nonhydrostatic pressures),[14,19] we do *not* observe superconductivity in $BaFe_2As_2$ at least up to 2.75 GPa. On the other hand, we do find that applied pressure strongly enhances T_c in the underdoped regime $0.02 \lesssim x \lesssim 0.051$. The pressure effect on T_c is very weak in the optimum and overdoped regimes, hence the *dome* of the superconducting region in the phase diagram extends toward x=0 under hydrostatic pressures.

The rest of this paper is organized as follows: in Sec. II, we describe experimental details. Our experimental results in ambient pressure and under hydrostatic pressure are described in Secs. III and IV, respectively, followed by summaries and conclusions in Sec. V.

II. EXPERIMENTAL METHODS

We grew Co-doped $BaFe_2As_2$ single crystals based on FeAs self-flux methods.[9] The samples were cleaved and cut into small pieces with typical dimensions of $2 \times 1 \times 0.15$ mm^3 for electrical transport measurements. We applied high pressures of up to 2.75 GPa using a compact hybrid pressure cell with a BeCu outer jacket and a NiCrAl inner core. Daphene oil 7373 and 99.99% purity Sn were used as a pressure transmitting medium and a pressure calibrating gauge, respectively. Sample contacts were made using silver epoxy for conventional four-lead ac-resistivity measurements. We employed a highly flexible, homemade ac-resistivity measurement rig to achieve high accuracy in

the resistivity measurements. The high-pressure cell was placed in a vacuum canister with helium exchange gas. All of the measurements reported in this paper were carried out while warming up the sample from the base temperature of 1.8 K. In order to ensure that thermal equilibrium was reached properly, we stabilized the temperature of the system before conducting the resistivity measurement at each temperature, instead of continuously ramping the temperature. We confirmed that measurements carried out in the warming cycle agree well with those in the cooling cycle for all of the measurements. We exercised these precautions because the heat capacity of the high-pressure cell is rather large, and the Cernox temperature sensor is attached to the exterior of the high-pressure cell. We estimate the upper bound for the potential inaccuracy in sample temperature at 0.5 K.

In this paper, we present the details of the resistivity measurements primarily for $x=0$, 0.02, 0.051, and 0.097. We refer readers to Ref. 21 for the additional details of measurements in $x=0.04$ and 0.082.

III. RESULTS IN AMBIENT PRESSURE

We begin our discussions with a summary of the resistivity data ρ_{ab} in ambient pressure, $P=0$, shown in Fig. 1(a). In the undoped sample with $x=0$, ρ_{ab} decreases suddenly below $T_{\mathrm{SDW}}=135$ K, in agreement with earlier reports.[2,22] The cause of this dramatic change has been identified as a first-order SDW phase transition accompanied by a structural phase transition from a high-temperature tetragonal to low-temperature orthorhombic structure.[2] We note that ρ_{ab} would increase below T_{SDW} if SDW energy gaps open for all branches of bands crossing the Fermi energy.[23] Instead, ρ_{ab} actually decreases below T_{SDW} in the undoped sample. We can understand this if we realize that gapless Fermi pockets remain below T_{SDW} in $BaFe_2As_2$ (Ref. 24); scattering of electrons associated with these Fermi pockets become much weaker below T_{SDW} because the long-range SDW order suppresses spin fluctuations.

Once we dope a few percent of Co into the Fe sites, however, the abrupt drop of ρ_{ab} is no longer observable, and ρ_{ab} exhibits a steplike increase.[21,25] We proposed earlier that the temperature derivative $d\rho_{ab}/dT$ of the resistivity data permits us to characterize the steplike anomaly.[21] We show the summary of the temperature dependence of $d\rho_{ab}/dT$ in Fig. 2. The minimum of $d\rho_{ab}/dT$ is clearly observable at $T_{\mathrm{SDW}}=100\pm1$ K for $x=0.02$. The justification for identifying the minimum of $d\rho_{ab}/dT$ as T_{SDW} is that our ^{75}As and ^{59}Co NMR measurements for the same batch of crystals reveal typical signatures of a second-order magnetic phase transition at the same temperature, including divergent behavior of the nuclear-spin-lattice relaxation rate $1/T_1$ and the onset of broadening of the NMR line shapes.[8,10] The enhancement of $1/T_1$ originates from the critical slowing down of the low-frequency components of spin fluctuations toward a second-order magnetic phase transition, while the NMR line broadening is due to the growth of spontaneous magnetization below a magnetic phase transition.

For higher doping levels with $x=0.04$ and 0.051, the resistivity upturn is less pronounced. By applying the same criterion based on the minimum of $d\rho_{ab}/dT$, we determined the SDW transition temperature as $T_{\mathrm{SDW}}=66\pm1$ K for $x=0.04$ and $T_{\mathrm{SDW}}=40\pm1$ K for $x=0.051$, respectively. Notice that the width of the SDW transition, as defined by the width of the peak (for $x=0$) or dip (for $x>0$) of $d\rho_{ab}/dT$ in Fig. 2(a), increases from 0.55 K for $x=0$ to 1.3 K ($x=0.02$), 3.5 K ($x=0.04$), and 13 K ($x=0.051$). The broadening of the SDW transition may be associated with the disorder induced by Co substitution.

We also observe a clear signature of a resistive superconducting transition for samples with $x=0.04$ or above. For example, the $x=0.04$ sample exhibits the onset of superconductivity at $T_c=11.0\pm0.5$ K. In what follows, we define the superconducting transition temperature T_c as the temperature where ρ_{ab} decreases by 10% from the extrapolated behavior of ρ_{ab} from higher temperature. We emphasize that none of our fundamental conclusions are sensitive to the way how we define T_c. For example, even if we define T_c as the temperature where $d\rho_{ab}/dT$ takes the maximum value, no qualitative aspects of Fig. 3 change. Interestingly, even the $x=0.02$ crystal shows a slight decrease in ρ_{ab} below 4 K. The observed decrease is very subtle in ambient pressure, but we will present evidence in Sec. IV that this drop is actually a precursor of superconductivity.

We summarize the concentration x dependence of T_{SDW} and T_c in the electronic phase diagram shown in Fig. 3. The underdoped samples with $x\lesssim0.051$ undergo successive SDW and superconducting phase transitions. The T_c reaches a maximum value of ~22.8 K in the optimally doped region for $0.06\lesssim x\lesssim0.082$. Although there is no SDW transition in the optimally doped regime, the NMR spin-lattice relaxation rate $1/T_1T$ is enhanced above T_c, providing evidence for the presence of residual antiferromagnetic spin fluctuations near T_c.[10,26] Once we enter the overdoped regime, T_c begins to decrease, and the NMR data no longer show evidence for enhanced antiferromagnetic spin fluctuations near T_c.[10] We will discuss the implications of the phase diagram in Sec. IV combined with the results of our measurements under hydrostatic pressure.

Among many puzzling aspects of the electronic properties of electron-doped $Ba(Fe_{1-x}Co_x)_2As_2$ is the temperature T and concentration x dependencies of ρ_{ab}. One can fit the overall temperature dependence of ρ_{ab} above T_{SDW} and T_c to a power-law behavior, $\rho_{ab}=A+BT^n$ with a constant background A.[21] The exponent n, as determined from the fit in the temperature range above 170 K so that we could apply the same fitting criterion for all samples, shows only a mild concentration dependence, $n=1.3-1.5$, above $x=0.04$, as summarized in Fig. 1(c). The observed exponent is very close to 4/3 or 3/2, typical values observed in some heavy Fermion systems[27] or overdoped high T_c cuprates.[28] It is not clear, however, if the assumption of the presence of a large temperature-independent background resistivity A is justifiable, especially in the underdoped regime; the residual resistance would increase with the Co concentration x if disorders induced by Co doping were the dominant cause. We also note that the extrapolation of the fit below 170 K poorly reproduces the data below ~100 K in superconducting samples. This is because ρ_{ab} asymptotes to a T-linear behavior near T_c. For example, if we employ the power-law fit

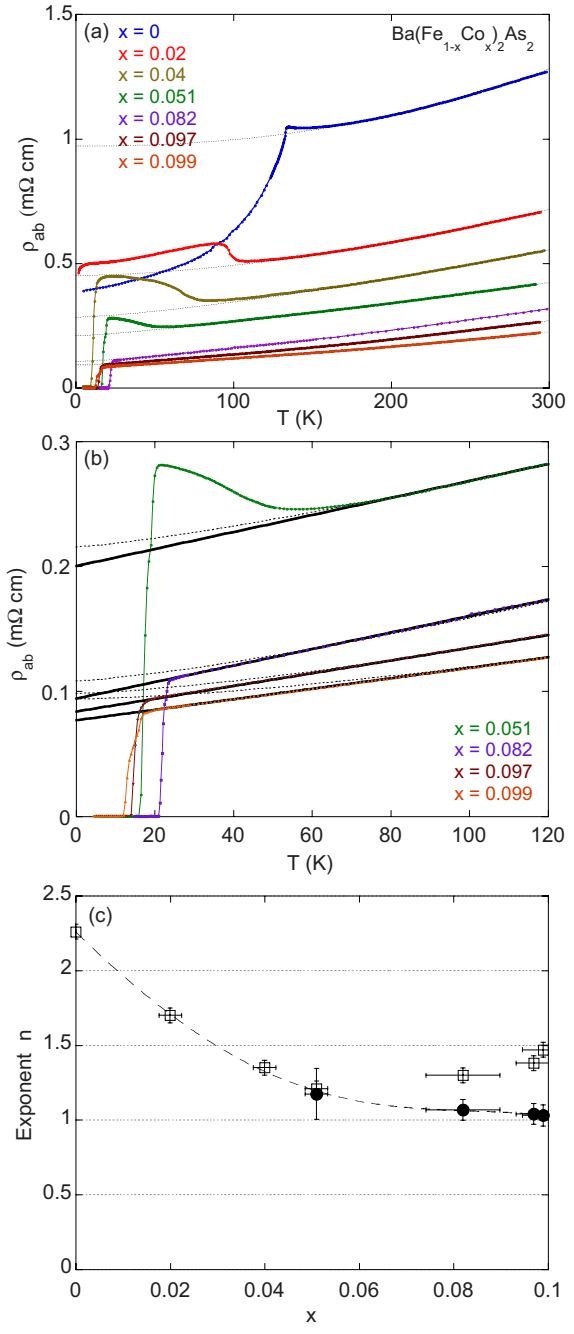

FIG. 1. (Color online) (a) The temperature dependence of the in-plane resistivity ρ_{ab} of $Ba(Fe_{1-x}Co_x)_2As_2$ single crystals in ambient pressure, $P=0$. Dotted curves are the best fits to an empirical power-law relation, $\rho_{ab}=A+BT^n$, above 170 K, where A and B are constants. The concentration dependence of n is summarized in panel (c) using open squares. (b) The same data shown on a magnified scale for the underdoped ($x=0.051$), optimal ($x=0.082$), and overdoped ($x=0.097, 0.099$) superconductors. Dotted curves represent the same power-law fit extrapolated from higher temperatures. Notice that the extrapolation markedly deviate from the data near T_c, where ρ_{ab} shows T-linear behavior, as shown by solid lines. (c) Open squares: the exponent n obtained from the free parameter fit of ρ_{ab} above 170 K. Filled circles: the exponent n obtained from the free parameter fit of ρ_{ab} below 100 K for $x=0.051$, 0.082, 0.097, and 0.099; notice that $n\sim1$ below ~100 K near the optimum doping.

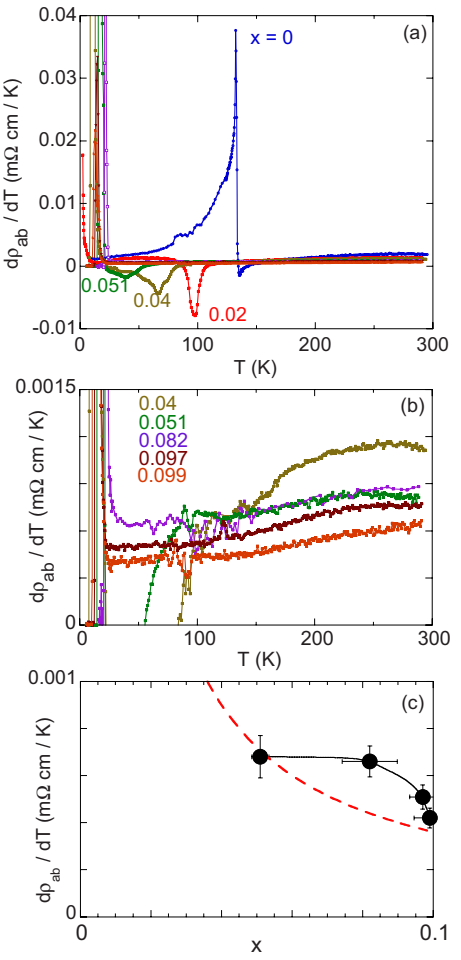

FIG. 2. (Color online) (a) The temperature dependence of the derivative of the in-plane resistivity, $d\rho_{ab}/dT$, for $Ba(Fe_{1-x}Co_x)_2As_2$ single crystals with $x=0$, 0.02, 0.04, and 0.051 in ambient pressure ($P=0$). (b) $d\rho_{ab}/dT$ for $x=0.04$ and above in a magnified scale. Notice that upon cooling, $d\rho_{ab}/dT$ levels off toward a constant value near ~100 K for $x=0.051$ and above, implying that $\rho_{ab}\propto T$. (c) Filled circles: the slope $d\rho_{ab}/dT$ in the $\rho_{ab}\propto T$ regime from T_c to ~100 K as obtained from the results in panel (b) for the superconducting samples with $x=0.051$ and above. The point for $x=0.051$ should be considered asymptotically valid value at low temperatures. Dashed curve represents $d\rho_{ab}/dT\sim1/x$, and does not account for the x dependence of $d\rho_{ab}/dT$ near T_c.

$\rho_{ab}=A+BT^n$ for the data points of $x=0.082$ below 100 K, we obtain $A=0.094$ mohm cm, $B=0.000\,66$ mohm cm/K^2, and $n=1.03$. In order to illustrate this point more clearly, we show the T-linear fit of ρ_{ab} below 100 K in Fig. 1(b). The derivative $d\rho_{ab}/dT$ in Fig. 2(b) also provides additional evidence for the nearly constant slope near T_c, i.e., T-linear behavior for $x=0.082$, 0.097, and 0.099. Figures 1(b) and 2(b) also suggest that ρ_{ab} asymptotes to the low-temperature T-linear behavior even for $x=0.051$, although the precursor of the SDW transition masks the T-linear behavior below ~70 K. We emphasize that these T-linear behaviors of superconducting samples are not consistent with canonical Fermi-liquid behavior, $\rho_{ab}\sim T^2$. This observation is supported by our earlier NMR measurements;[10,26] we recall that ^{75}As NMR results in the T-linear regime do not satisfy the

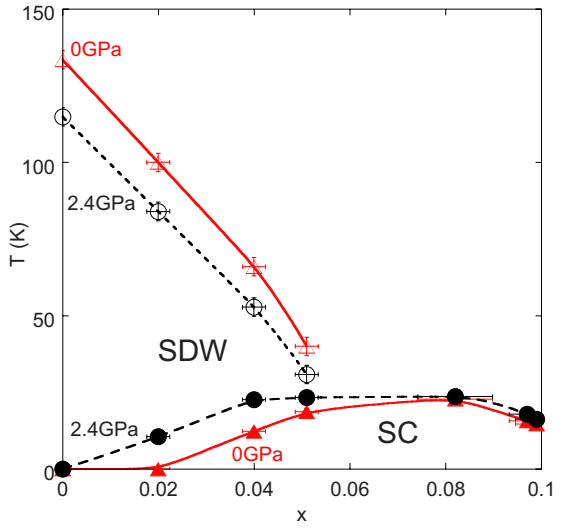

FIG. 3. (Color online) The SDW-SC (superconductivity) phase diagram of $Ba(Fe_{1-x}Co_x)_2As_2$ for $P=0$ (triangles) and 2.4 GPa (circles). Open and filled symbols are used to represent T_{SDW} and T_c, respectively.

Korringa law, $1/T_1T \propto [K_{spin}]^2$, expected for a Fermi liquid[10,26] (K_{spin} is the spin contribution to the NMR Knight shift, which is proportional to the uniform spin susceptibility).

In order to quantify the systematic variation of ρ_{ab}, we summarize the x dependence of ρ_{ab} at 290 K in Fig. 4(a). ρ_{ab} decreases monotonically with x. To better understand the systematic trend, we also plot the in-plane conductivity $\sigma_{ab}(=1/\rho_{ab})$ in Fig. 4(b). The latter suggests that σ_{ab} at 290 K increases in proportion to x, $\sigma_{ab}(x)=\sigma_{ab}(0)+Cx$ where C is a constant. We found that the concentration dependence of σ_{ab} at a fixed temperature above 150 K shows analogous linear dependence on x as long as all samples remain paramagnetic. It is well known that similar linear x dependence of σ_{ab} was also observed in the high T_c cuprates for a broad concentration range.[28–30]

In the case of the high T_c cuprate $La_{2-x}Sr_xCuO_4$, ρ_{ab} exhibits T-linear behavior over a broad temperature range up to

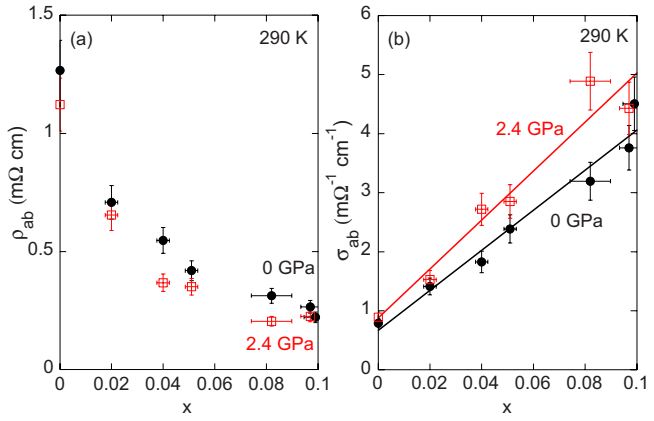

FIG. 4. (Color online) (a) The concentration dependence of the in-plane resistivity ρ_{ab} at 290 K for $P=0$ (filled circles) and $P=2.4$ GPa (open squares). (b) The conductivity $\sigma_{ab}=1/\rho_{ab}$ at 290 K. Solid lines represent the best linear fits to the data.

as high as ~1000 K and for a broad hole-concentration range from $x=0.01$ to 0.22.[30] This T-linear behavior in cuprates may be caused by, among other possibilities, the quantum criticality as discussed in Ref. 31. The persistence of the T-linear behavior to such high temperatures implies that the fundamental energy scale which dictates the electronic properties of high T_c cuprates is large (e.g., the Cu-Cu superexchange interaction J is as large as ~1500 K in undoped La_2CuO_4). In contrast, in the present case, the T-linear behavior is observed only below ~100 K and only near the optimal composition $x \sim 0.082$, as shown in Fig. 1. The fact that the T-linear behavior breaks down above ~100 K suggests that the fundamental energy scale of the electronic properties of $Ba(Fe_{1-x}Co_x)_2As_2$ is relatively low.

Another important distinction is the concentration dependence of the slope. In cuprates, the slope is roughly inversely proportional to the doped hole concentration, i.e., $d\rho_{ab}/dT \sim 1/x$ in the T-linear regime.[30] This implies that each hole in the CuO_2 planes of the high T_c cuprates contributes to the in-plane conductivity $\sigma_{ab}(=1/\rho_{ab})$ by the same amount, regardless of the level of doping. In the present case, however, the low-temperature slope in the T-linear region does not vary as $\sim 1/x$, as shown in the Fig. 2(c). Instead, $d\rho_{ab}/dT$ is roughly constant in the optimally doped regime and begins to decrease very rapidly once we enter the overdoped regime above $x=0.082$. In fact, upon further increasing x, $BaCo_2As_2$ with $x=1$ has a Fermi-liquid-like ground state and satisfies $\rho_{ab} \sim T^2$ below ~70 K.[32,33] The latter implies that $d\rho_{ab}/dT \sim 0$ with decreasing temperature for $x=1$. Recent studies suggest that this crossover into the Fermi-liquid-like ground state with $\rho_{ab} \sim T^2$ takes place around $x=0.2$.[11–13]

IV. PRESSURE EFFECTS

In Fig. 5, we summarize representative results of resistivity measurements under hydrostatic pressures for undoped $x=0$, lightly doped $x=0.02$, underdoped $x=0.051$, and overdoped $x=0.097$ samples. We refer readers to our earlier report for the details of the measurements on underdoped $x=0.04$ and optimally doped $x=0.082$ samples.[21] In all cases except for $x=0.02$, ρ_{ab} does not show major qualitative changes under hydrostatic pressure. The magnitude of ρ_{ab} decreases by ~20% from 0 GPa to ~2.4 GPa, but the empirical relation for the concentration dependence, $\sigma_{ab}(x)=\sigma_{ab}(0)+Cx$, still holds with a ~20% larger value of C, as shown in Fig. 4(b). The exponent n from the fit to $\rho_{ab}=A+BT^n$ is also comparable between $P=0$ and 2.4 GPa.[21] In the case of $x=0.02$, the aforementioned decrease in resistivity near the base temperature is significantly enhanced under pressures. In 2.4 GPa, resistivity begins to decrease below ~10.5 K and ρ_{ab} approaches zero at 1.8 K. As shown in Fig. 6, we also confirmed that application of a 9 T magnetic field suppresses the onset of the resistivity drop while NMR measurements[8] reveal no additional magnetic anomaly around ~10 K or below. We therefore conclude that even the lightly electron-doped $x=0.02$ crystal has a resistive superconducting transition under pressures.

How does hydrostatic pressure affect the phase-transition temperatures T_{SDW} and T_c? In the case of undoped $BaFe_2As_2$,

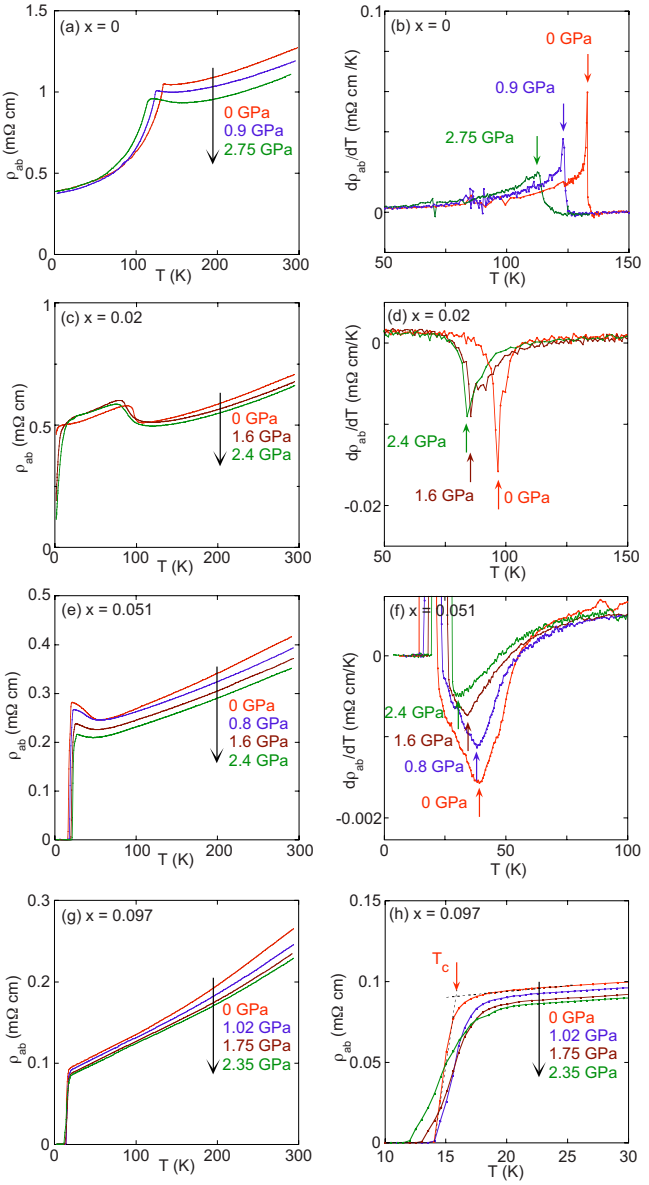

FIG. 5. (Color online) Left panels: in-plane resistivity ρ_{ab} under pressure for various values of Co concentration x. The upper right panels (b), (d), and (f) show the derivative of the in-plane resistivity $d\rho_{ab}/dT$. The bottom right panel (h) shows the resistive superconducting transition for $x=0.097$ under various pressures.

our ρ_{ab} data in Fig. 5(a) and its derivative $d\rho_{ab}/dT$ in Fig. 5(b) clearly show progressive suppression of T_{SDW} from 135 K in 0 GPa to 114 K in 2.75 GPa. The extremely sharp peak of $d\rho_{ab}/dT$ at $T_{\mathrm{SDW}}=135$ K becomes broader under pressure, and the sharp peak is no longer observable in 2.75 GPa. This may be an indication that the first-order nature of the phase transition at T_{SDW} in 0 GPa becomes gradually weaker under pressure. However, we cannot entirely rule out an alternate scenario in which the applied pressure has a mild distribution due to the freezing of the pressure medium, etc., and therefore T_{SDW} itself has a small distribution under pressures, especially at $P=2.75$ GPa. A distribution of T_{SDW} over ~5 K would easily mask the sudden nature of the first-order phase transition and make the transition appear to be of the second order.

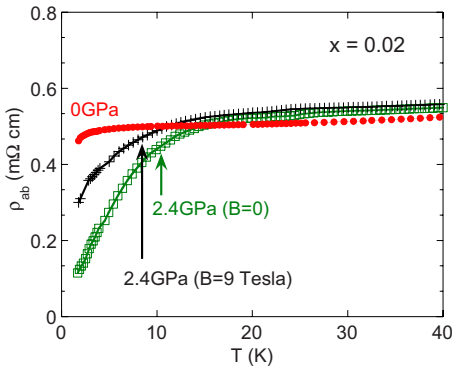

FIG. 6. (Color online) A magnified view of the resistivity data of $x=0.02$ sample in ambient pressure (filled circles), 2.4 GPa and zero external magnetic field $B=0$ (open squares), and 2.4 GPa and $B=9$ Tesla along the ab plane (crosses). Notice that the application of 9 Tesla magnetic field strongly suppresses the resistivity drop. Arrows mark the T_c.

Another important aspect of our ρ_{ab} data for the undoped $BaFe_2As_2$ is that we find no hint of a resistive superconducting transition up to at least 2.75 GPa. In contrast with our results, earlier superconducting quantum interference device (SQUID) measurements detected diamagnetic Meissner signals of a superconducting transition with T_c as high as 29 K in $BaFe_2As_2$ above a critical pressure $P_c \sim 2.8$ GPa applied by diamond-anvil cell.[14] A subsequent report on resistivity measurements in nonhydrostatic pressure applied by a Bridgman cell also detected strong suppression of resistivity above a comparable P_c although zero resistivity was never observed.[19] In the present case, we cannot rule out the possibility that our maximum hydrostatic pressure of 2.75 GPa ($<P_c$) is somewhat too low to induce superconductivity. Our compact hydrostatic high-pressure cell risks damage or even a catastrophic failure at ~3 GPa or higher. Accordingly, we have not explored the pressure range above 2.8 GPa, and the role played by the hydrostaticity of applied pressure above 2.8 GPa remains to be seen. However, it is worth pointing out that our ρ_{ab} data in 2.75 GPa shows a robust signature of an SDW transition at $T_{\mathrm{SDW}}=114$ K; it seems highly unlikely that bulk superconductivity suddenly sets in under hydrostatic pressure at $P_c \sim 2.8$ GPa unless a structural phase transition takes place between 2.75 and 2.8 GPa.

Next, we turn our attention to the interplay between Co doping and applied pressure. We summarize T_{SDW} and T_c as a function of hydrostatic pressure in Figs. 7(a) and 7(b), respectively. Figure 7(c) summarizes the pressure coefficient, dT_{SDW}/dP and dT_c/dP, for various Co doping levels based on the linear fits of the data points in Figs. 7(a) and 7(b). The results in Figs. 7(a) and 7(c) clearly establish that the pressure-induced suppression of T_{SDW} becomes progressively weaker as we increase the Co concentration from $x=0$ to 0.051. On the other hand, Figs. 7(b) and 7(c) show that hydrostatic pressure always enhances T_c but the sensitivity of T_c on pressure depends strongly on the Co concentration x. dT_c/dP reaches as large as +4.3 K/GPa for $x=0.02-0.04$ but dT_c/dP decreases to $\leq +1$ K/GPa in the optimum and overdoped regimes. It is not clear why the pressure effect on T_c becomes so weak for $x=0.082$ or above. Another remark-

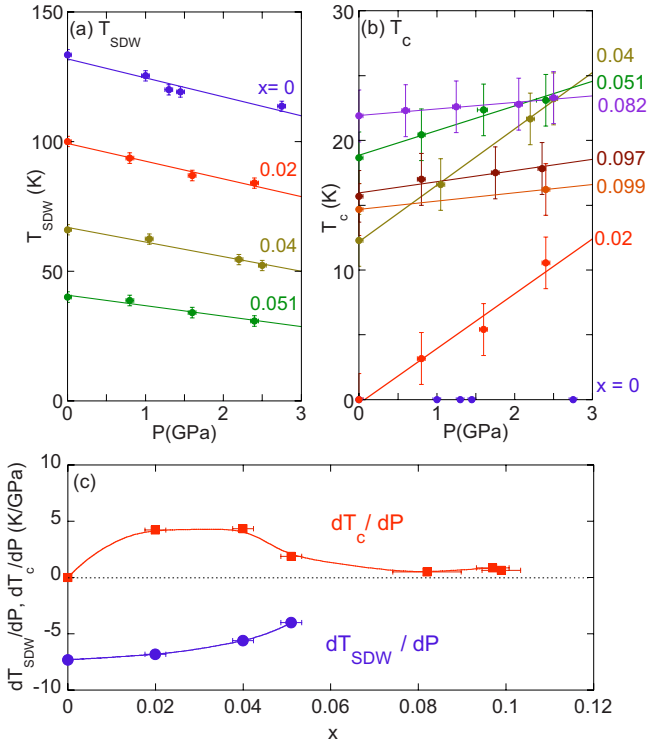

FIG. 7. (Color online) The pressure P dependence of (a) T_{SDW} and (b) T_c. Solid lines are the best linear fits. (c) The pressure coefficient dT_c/dP and dT_{SDW}/dP as a function of the Co concentration x. Solid curves are guides for the eyes.

able point from Fig. 7(c) is that the magnitude of *both* dT_{SDW}/dP and dT_c/dP decrease strongly near $x \sim 0.06$. In other words, the effects of pressure on T_c and T_{SDW} become weak near $x \sim 0.06$. These trends suggest the existence of a crossover in the electronic properties near $x \sim 0.06$. This finding may be related to a recent report on the crystal structure which showed that $Ba(Fe_{1-x}Co_x)_2As_2$ does not undergo a high-temperature tetragonal to low-temperature orthorhombic structural phase transition in the concentration range $x \gtrsim 0.06$.[34]

In passing, it is worth noting that the pressure effects on T_c do not seem to obey a simple universal behavior in other systems either and what dictates the pressure-induced change in T_c is not clear. For example, in the case of the $(Ba_{1-x}K_x)Fe_2As_2$ system with $x=0.45$, T_c decreases smoothly with pressure up to 2 GPa at a rate $dT_c/dP \sim -2.1$ K/GPa.[35] On the other hand, for the $La(O_{1-x}F_x)FeAs$ system $T_c \sim 28$ K sharply increases to 43 K with pressure up to 3 GPa at an average rate $dT_c/dP \sim +5$ K/GPa but application of higher pressure suppresses T_c.[36]

V. SUMMARY AND CONCLUSIONS

By linearly interpolating data points in Figs. 7(a) and 7(b) at $P=2.4$ GPa, we construct the electronic phase diagram of $Ba(Fe_{1-x}Co_x)_2As_2$ under pressure at $P=2.4$ in Fig. 3. Application of a hydrostatic pressure of 2.4 GPa suppresses T_{SDW} by 10–19 K for all samples with a SDW transition. On the other hand, applied pressures enhance T_c dramatically only in the underdoped region while affecting T_c little in the optimum and overdoped regimes. Accordingly, the optimally doped regime with $T_c(2.4\ \mathrm{GPa}) \sim 23.6$ K extends to as low as $x=0.04-0.051$. Also notice that the optimally doped region emerges when the magnetic phase boundary T_{SDW} intersects the dome of the superconducting phase near $x \sim 0.05$ in $P=2.4$ GPa. In the case of ambient pressure, the intersection is located at a somewhat higher value near $x \sim 0.06$.[10–13]

One can take several different views on the phase diagram in Fig. 3. One possible scenario is that the SDW and superconducting phases compete each other. In this viewpoint, one can attribute the extension of the optimum T_c region to $x=0.04-0.05$ in 2.4 GPa as a consequence of the suppression of the SDW instability by pressure. One can also take a completely opposite viewpoint. As demonstrated in our earlier NMR measurements of $1/T_1T$, paramagnetic spin fluctuations are enhanced near the SDW-superconductor phase boundary (see Fig. 5 of Ref. 10). That is, if we traverse the phase diagram near $T=0$ from the superconducting phase $x \sim 0.1$ toward $x=0$, low-frequency antiferromagnetic spin fluctuations as a function of x would diverge at $x_c \sim 0.06$ in $P=0$ GPa when we hit the boundary with the SDW phase, i.e., *a quantum phase transition* at x_c from the superconducting to SDW ground state.

In this second scenario, our phase diagram in Fig. 3 might imply that enhanced quantum spin fluctuations near x_c are the key to the superconducting mechanism. We recall that an analogous scenario involving quantum criticality has been debated extensively in the context of high T_c cuprates since the early 1990's (Refs. 31, 37, and 38) and more recently in the context of pressure-induced superconductivity in heavy Fermions.[39,40] The recent finding that application of hydrostatic pressure enhances both T_c (Refs. 41–43) and antiferromagnetic spin fluctuations in FeSe (Ref. 44) renders additional support to this second scenario, because spin fluctuations would be suppressed by pressure if superconductivity genuinely competes with the SDW instability.

On the other hand, one may need to be somewhat cautious in the debate over the cooperation or competition between superconductivity and SDW in the present case of $Ba(Fe_{1-x}Co_x)_2As_2$ because the structural phase boundary between the tetragonal and orthorhombic phases terminates near $x=0.06$.[34] We cannot rule out the possibility that subtle changes in the crystal structure turn off the SDW order rather suddenly and switch on superconductivity. In this third scenario, x_c decreases from ~ 0.06 in 0 GPa to ~ 0.05 in 2.4 GPa as a consequence of the shift of the tetragonal-orthorhombic structural boundary to $x \sim 0.05$ under pressure. Further structural studies under pressure are required to test the scenario.

ACKNOWLEDGMENTS

We thank D. J. Singh for helpful discussions. The work at McMaster was supported by NSERC, CFI, and CIFAR. Research at ORNL was sponsored by Division of Materials Sciences and Engineering, Office of Basic Energy Sciences, (U.S.) Department of Energy.

[1] Y. Kamihara, T. Watanabe, M. Hirano, and H. Hosono, J. Am. Chem. Soc. **130**, 3296 (2008).
[2] Q. Huang, Y. Qiu, W. Bao, M. A. Green, J. W. Lynn, Y. C. Gasparovic, T. Wu, G. Wu, and X. H. Chen, Phys. Rev. Lett. **101**, 257003 (2008).
[3] K. Kitagawa, N. Katayama, K. Ohgushi, M. Yoshida, and M. Takigawa, J. Phys. Soc. Jpn. **77**, 114709 (2008).
[4] A. Jesche *et al.*, Phys. Rev. B **78**, 180504(R) (2008).
[5] F. Ronning, T. Klimczuk, E. D. Bauer, H. Volz, and J. D. Thompson, J. Phys.: Condens. Matter **20**, 322201 (2008).
[6] N. Ni, S. Nandi, A. Kreyssig, A. I. Goldman, E. D. Mun, S. L. Bud'ko, and P. C. Canfield, Phys. Rev. B **78**, 014523 (2008).
[7] M. Rotter, M. Tegel, and D. Johrendt, Phys. Rev. Lett. **101**, 107006 (2008).
[8] F. L. Ning, K. Ahilan, T. Imai, A. S. Sefat, R. Jin, M. A. McGuire, B. C. Sales, and D. Mandrus, Phys. Rev. B **79**, 140506(R) (2009).
[9] A. S. Sefat, R. Jin, M. A. McGuire, B. C. Sales, D. J. Singh, and D. Mandrus, Phys. Rev. Lett. **101**, 117004 (2008).
[10] F. L. Ning, K. Ahilan, T. Imai, A. S. Sefat, R. Jin, M. A. McGuire, B. C. Sales, and D. Mandrus, J. Phys. Soc. Jpn. **78**, 013711 (2009).
[11] N. Ni, M. E. Tillman, J. Q. Yan, A. Kracher, S. T. Hannahs, S. L. Bud'ko, and P. C. Canfield, Phys. Rev. B **78**, 214515 (2008).
[12] J.-H. Chu, J. G. Analytis, C. Kucharczyk, and I. R. Fisher, Phys. Rev. B **79**, 014506 (2009).
[13] X. F. Wang, T. Wu, R. H. Liu, H. Chen, Y. L. Xie, and X. H. Chen, New J. Phys. **11**, 045003 (2009).
[14] H. Alireza, B. C. Ko, H. L. Gillett, J. Petrone, R. J. Cole, G. G. Lonzarich, and W. F. Sebastian, J. Phys.: Condens. Matter **21**, 012208 (2009).
[15] M. S. Torikachvili, S. L. Bud'ko, N. Ni, and P. C. Canfield, Phys. Rev. Lett. **101**, 057006 (2008).
[16] T. Park, E. Park, H. Lee, T. Klimczuk, E. D. Bauer, F. Ronning, and J. D. Thompson, J. Phys.: Condens. Matter **20**, 322204 (2008).
[17] K. Igawa, H. Okada, H. Takahashi, S. Matsuishi, Y. Kamihara, M. Hirano, H. Hosono, K. Matsubayashi, and Y. Uwatoko, J. Phys. Soc. Jpn. **78**, 025001 (2009).
[18] H. Kotegawa, H. Sugawara, and H. Tou, J. Phys. Soc. Jpn. **78**, 013709 (2009).
[19] H. Fukazawa, N. Takeshita, T. Yamazaki, K. Kondo, K. Hirayama, Y. Kohori, K. Miyazawa, H. Kito, H. Eisaki, and A. Iyo, J. Phys. Soc. Jpn. **77**, 105004 (2008).
[20] C. W. Chu and B. Lorenz, arXiv:0902.0809 (unpublished).
[21] K. Ahilan, J. Balasubramaniam, F. L. Ning, T. Imai, A. S. Sefat, R. Jin, M. A. McGuire, B. C. Sales, and D. Mandrus, J. Phys.: Condens. Matter **20**, 472201 (2008).
[22] M. Rotter, M. Tegel, D. Johrendt, I. Schellenberg, W. Hermes, and R. Pottgen, Phys. Rev. B **78**, 020503(R) (2008).
[23] D. Jerome and H. Schultz, Adv. Phys. **31**, 299 (1982).
[24] D. J. Singh, Phys. Rev. B **78**, 094511 (2008).
[25] A. S. Sefat, A. Huq, M. A. McGuire, R. Jin, B. C. Sales, D. Mandrus, L. M. D. Cranswick, P. W. Stephens, and K. H. Stone, Phys. Rev. B **78**, 104505 (2008).
[26] F. L. Ning, K. Ahilan, T. Imai, A. S. Sefat, R. Jin, M. A. McGuire, B. C. Sales, and D. Mandrus, J. Phys. Soc. Jpn. **77**, 103705 (2008).
[27] J. L. Sarrao, L. A. nad Morales, J. D. Thompson, B. L. Scott, G. R. Stewart, F. Wastin, J. Rebizant, P. Boullet, E. Colineau, and G. H. Lander, Nature (London) **420**, 297 (2002).
[28] H. Takagi, B. Batlogg, H. L. Kao, J. Kwo, R. J. Cava, J. J. Krajewski, and W. F. Peck, Phys. Rev. Lett. **69**, 2975 (1992).
[29] Y. Ando, G. S. Boebinger, A. Passner, T. Kimura, and K. Kishio, Phys. Rev. Lett. **75**, 4662 (1995).
[30] Y. Ando, S. Komiya, K. Segawa, S. Ono, and Y. Kurita, Phys. Rev. Lett. **93**, 267001 (2004).
[31] A. V. Chubukov and S. Sachdev, Phys. Rev. Lett. **71**, 169 (1993).
[32] A. S. Sefat, D. J. Singh, R. Jin, M. A. McGuire, B. C. Sales, and D. Mandrus, Phys. Rev. B **79**, 024512 (2009).
[33] A. S. Sefat, D. J. Sing, R. Jin, M. A. McGuire, B. C. Sales, F. Ronning, and D. Mandrus, arXiv:0903.0629, Physica C (to be published).
[34] C. Lester, J.-H. Chu, J. G. Analytis, S. Capelli, A. S. Erickson, C. L. Condron, M. F. Tony, I. R. Fisher, and S. M. Hayden, Phys. Rev. B **79**, 144523 (2009).
[35] M. S. Torikachvili, S. L. Bud'ko, N. Ni, and P. C. Canfield, Phys. Rev. B **78**, 104527 (2008).
[36] H. Takahashi, K. Igawa, K. Arii, Y. Kamihara, M. Hirano, and H. Hosono, Nature (London) **453**, 376 (2008).
[37] T. Imai, C. P. Slichter, K. Yoshimura, K. Katoh, and K. Kosuge, Physica B **197**, 601 (1994).
[38] A. Sokol and D. Pines, Phys. Rev. Lett. **71**, 2813 (1993).
[39] S. S. Saxena *et al.*, Nature (London) **406**, 587 (2000).
[40] N. D. Mathur, F. M. Grosche, S. R. Julian, I. R. Walker, I. R. Freye, R. K. W. Haselwimmer, and G. G. Lonzarich, Nature (London) **394**, 39 (1998).
[41] Y. Mizuguchi, F. Tomioka, S. Tsuda, T. Yamaguchi, and Y. Takano, Appl. Phys. Lett. **93**, 152505 (2008).
[42] S. Medvedev *et al.*, arXiv:0903.2143 (unpublished).
[43] S. Margadonna, Y. Takabayashi, Y. Ohishi, Y. Mizuguchi, Y. Takano, T. Kagayama, T. Nakagawa, M. Takata, and K. Prassides, arXiv:0903.2204 (unpublished).
[44] T. Imai, K. Ahilan, F. L. Ning, T. M. McQueen, and R. J. Cava, Phys. Rev. Lett. **102**, 177005 (2009).